The Egyptian Journal of Hospital Medicine (July 2019) Vol. 76 (1), Page 3299-3306

Histological Study of Effect of Exposure to Emamectin Benzoate on the Kidney of Adult Male Albino Rats and the Possible Protective Effect of Ginger Nanoparticles

Mervat Shaker Mehanna, Fatma Al-Zahraa Nabil Mohammed Al-Shahed, Marwa Kamal Taha
Department of Histology, Faculty of Medicine for Girls, Al-Azhar University
Corresponding author: **Marwa Kamal Taha, email:** Marwa_histo@yahoo.com

ABSTRACT

Background: pesticides are pivotal for pest control. However, due to their cumulative nature humans are vulnerable to daily sub-lethal exposure with increased risk for clinical disorders including kidney diseases. Oxidative stress is the main proposed mechanism for pesticides biohazards. **Aim of this study:** to clarify the effect of exposure to emamectin benzoate (EMB) on structure and ultrastructure of the kidney of adult male albino rats and the possible protective effect of aqueous ginger nanoparticles extract (GNE) on these changes.

Materials and Methods: four groups were incorporated in this study, six animals each. GI: control group; GII: received aqueous GNE (100 mg/kg/d); GIII: received EMB (5 mg/kg/d); GIV: received EMB and aqueous GNE. Initial/final body weight (BW) variations and biochemical tests of serum creatinine (sCr) and blood urea nitrogen (BUN) were assessed. After one month, both kidneys from all groups were excised under anesthesia and prepared for light and electron microscopic assessment. The results were statistically evaluated. **Results:** comparing mean final BW among all groups revealed insignificant decrease in BW of GIII. There was a significant increase in the mean final sCr and BUN in GIII which was improved in GIV ($p< 0.001$). There was a significant increase in area percent of both collagen fibers deposition and Bax immune-expression in GIII which was markedly diminished in GIV ($p< 0.001$). Morphologic alternations were detected in kidney of rats of GIII which was ameliorated in GIV. **Conclusion:** EMB altered kidney morphology and aqueous GNE exerted an ameliorative effect.

Keywords: kidney, EMB, nanoparticles, ginger.

INTRODUCTION

Pesticides are used for pest management for agriculture and health care. Because of their unwise use, classical pesticides threaten biodiversity, food and water resources. Thus, biopesticides have become a reasonable alternative [(1)].EMB is a broad spectrum biopesticide, belongs to avermectins (AVMs) that are widely used as pesticides as well as in human and veterinary medicine. Although once considered safer, EMB potential hazard to the environment and human well-being was recently revealed with induction of oxidative stress is the main proposed mechanism [(2)].Kidney diseases constitute heavy burden upon economy and health care system. The commonest risk factors are diabetes mellitus, hypertension and obesity. However, lately, chronic kidney disease of unknown cause reported from different countries including Egypt has drawn the attention. It is a multifactorial, but the most accepted hypothesis is genetically susceptible individuals with unfavourable work conditions-e.g. heat stress and dehydration associated with exposure to agrochemicals i.e. pesticides and fertilizers- are at major risk [(3)].Ginger *(Zingiber officinale)* has long been used in several forms to alleviate various complaints. Its basic elements are famous for their antioxidant, anti-inflammatory, cytoprotective, hepatoprotective and renoprotective bioactivity [(4)]. Nanotechnology is a promising emerging science. Its privilege is alternating substance characteristics via converting its size to nanoscale. Milling herbs to nanoscale increase their exposed surface area and porosity, hence, enhancing their active compounds solubility and bioavailability [(5)].

MATERIAL AND METHODS

Emamectin Benzoate (Hypnose 5% SG, SAFA TARIM. A.S, Turkey) in the form of white powder, was generously provided by Agricultural Research Centre, Plant Protection Research Institute; El-Dokki, Giza, Egypt.

Preparation of ginger nanoparticles (GN):

Plant material:

Dried Nigerian white ginger rhizomes *(Zingiber officinale)* were purchased from local market, Egypt. They were ground using hammer mill at 2890 rpm, sieved using a 250µm sieve, then was brought down to nanosize by dry milling, where 20gm of dried ginger powder was introduced to the planetary ball mill device (Retsch PM 400, Germany) with 2 mm zirconia beads milled for 4 hours at 550 rpm [(5)], performed at the Egyptian Petroleum Research Institute-Nanotechnology Centre; Nasr City,Cairo,Egypt.

Preparation of the extract:

The aqueous extract was freshly prepared according to the method of **Norhidayah *et al.*** [(5)], then filtrated through filter paper (wattman-5). The filtrate was then collected and stored at 4°C until used.

Characterization of GN:

Dynamic light scattering (DLS) for particles size and potential:

Assessed by using Malvern Zetasizer ZS (Malvern, UK); performed at Egyptian Petroleum

Received:5/4/2019
Accepted:4/5/2019

Research Institute-Nanotechnology Centre; Nasr City, Cairo, Egypt.

Particles morphology:

Assessed by using transmission electron microscope (TEM), GN were suspended in distilled water(DW) in 1.5 mL eppendorf, centrifuged for 5 minutes, then one drop was placed on carbon coated grid, left to dry on filter paper at room temperature, and stained with 2%phosphotungstic acid. Examination under JOEL electron microscope (JEM-2100, Japan) was performed at Electron Microscopy Unit at National Research Centre; El-Dokki, Giza, Egypt.

Animals and experimental model:

The presented study included 24 adult male albino rats weighting 159-161gm. They were allowed to acclimatize for one week prior to the experiment and **they were handled in respect to the guidelines and ethics of animal protocol of Faculty of Medicine Al-Azhar University, Cairo, Egypt.** They were kept in well ventilated cages, 12 hours light/dark cycle, room temperature was maintained at 23 ± 2°C and allowed to access freely to water and commercial rat food, at the animal house of Faculty of Medicine, Cairo University. The study was carried over one month. The animals were categorized into four groups, six animals each:

GI (control group): received a corresponding volume of DW only in a dose of 1 ml/kg/d by gastric gavage [(6)].

GII (aqueous GNE control group): received aqueous GNE only in a dose of (100 mg/kg/d) by gastric gavage [(7)].

GIII (EMB group): received freshly prepared EMB in DW only in a dose of 5 mg/kg/d by gastric gavage [(8)].

GIV (EMB and aqueous GNE group): received aqueous GNE prior to EMB in the above mentioned doses. Animal's body weight was assessed prior to the study and just before sacrifice.

Biochemical assessment:

At the end of one month, the animals were gently handled under light anaesthesia and blood samples were collected from retro-orbital venous sinus by using capillary glass tube, centrifuged (2,500 rpm) for 20 minutes; then serum was collected for assessment of initial/final sCr and BUN.

Histological study:

For light microscopic (L/M) study, sections of 5 μm thickness were stained with sirius red to assess collagen fibres deposition [(9)]. Immunohistochemistry was performed at Cancer Institute-Cairo University, according to the method of **Kiernan** [(9)] to detect Bax protein immune-expression in renal cortex. Bax is a cytosolic protein involved in induction of intrinsic pathway of apoptosis [(10)]. The other kidney was processed for the electron microscopic (E/M) study. 1 μm semithin sections were obtained using LKB ultramicrotom and stained with toluidine blue for L/M examination prior to final trimming [(11)]. Ultrathin sections were examined under JEOL TEM (100s, Japan) at 60 kV accelerating voltage, at Histology Department, Faculty of Medicine, Al-Azhar University.

Morphometry:

Quantitative analysis of area percent (%) were assessed in six non-overlapping fields/group randomly selected in a standard measuring frame at 400X magnification for detection of collagen fibres deposition; after exclusion of blood vessels and medullary tissue [(12)]; as well as Bax expression in renal cortical tissue. It was performed using Leica QWin plus analyzer computer system. Morphometry was performed at Pathology Department, Faculty of Dentistry, Cairo University.

Statistical design:

Data were statistically evaluated using statistical package for social science (SPSS), Version 21. The quantitative results were expressed as mean ± standard error and mean standard deviation. The different results were evaluated statistically using: ANOVA (Analysis of Variance): for comparison of quantitative data of more than two groups. p-value: is significant if < 0.001.

RESULTS

DLS results:

The obtained GN specimen was a mixture of 98.5% small particles (75.59nm) and 1.5% large particles (413.4nm) **(Figure 1a)**. The specimen Zeta potential was -25.6mV **(Figure 1b)**.

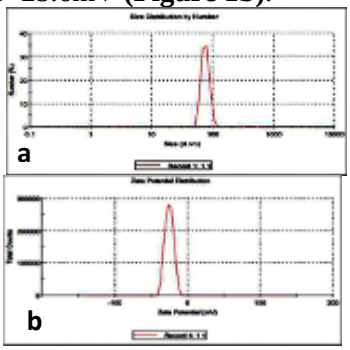

Figure 1: measurements of GN size and potential

Particles morphology:

Homogenous GN distribution as well as agglomeration was observed in **figure 2**.

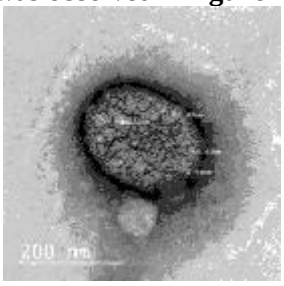

Figure 2: TEM micrographs showing GN size and distribution.

Body weight:

There was an insignificant difference of mean initial BW among the four groups. Comparing mean

final BW among all groups revealed insignificant decrease in GIII (205.5± 10.1) **(Histogram 1)**.

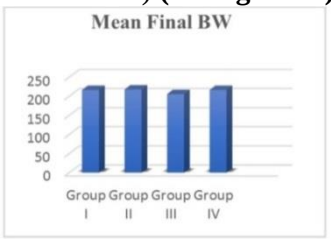

Histogram 1: showing comparison of final BW among the four groups.

Biochemical results:

Comparison of mean initial sCr and BUN revealed insignificant difference among the four groups. Comparing mean final sCr and BUN revealed a significant increase in mean final sCr and BUN (1.42±0.05), (28.4±2.06) respectively in GIII, and improvement of mean final sCr and BUN (1.37±0.05), (24.4±0.7) respectively in GIV**(Histogram 2a,b)**.

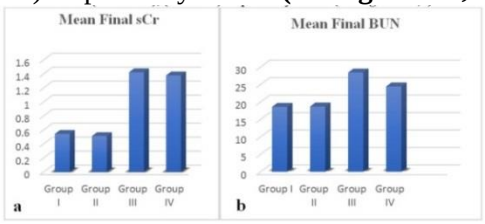

Histogram 2: showing comparison of final: **a)** sCr ***b)*** BUN among the four groups.

L/M findings:

There was positive sirius red reaction in renal corpuscles and tubular basement membrane in GI and GII**(Figure3a,b)**.Whereas,in GIII there was a marked increase in collagen fibres deposition around renal corpuscles as compared to GIand GII **(Figure3c)**, which was markedly reduced in GIV**(Figure 3d)**. The results were morphometrically evaluated**(Histogram 3a)**.

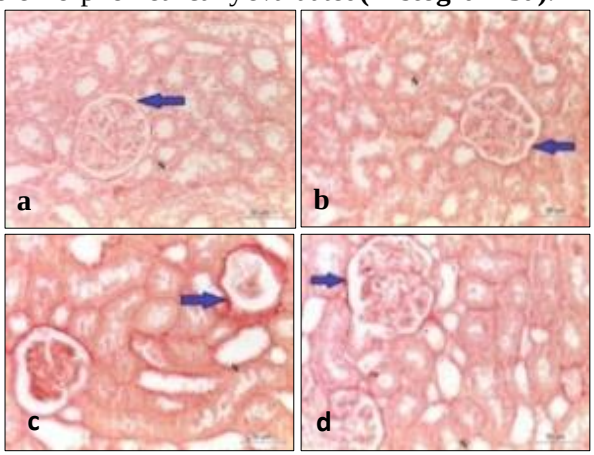

Figure 3: photomicrographs of sections of renal cortex of the adult male albino rats **a)** GI, **b)** GII revealing: positive sirius red reaction around renal corpuscles (blue arrow). **c)** GIII revealing: marked increase in collagen fibers deposition around renal corpuscles (blue arrow). **d)** GIV revealing: markedly reduced collagen fibers deposition around renal corpuscles (blue arrow). **(Sirius red X400)**

Immunohistochemically, there was negative Bax immunoreactivity in glomerular cells in GI and GII **(Figure 4a, b)**. While in GIII, glomerular cells showed strong positive immunoreactivity**(Figure 4c)**, that was significantlyreduced in GIV**(Figure4d)**.Theresultswere morphometrically evaluated**(Histogram3b)**.

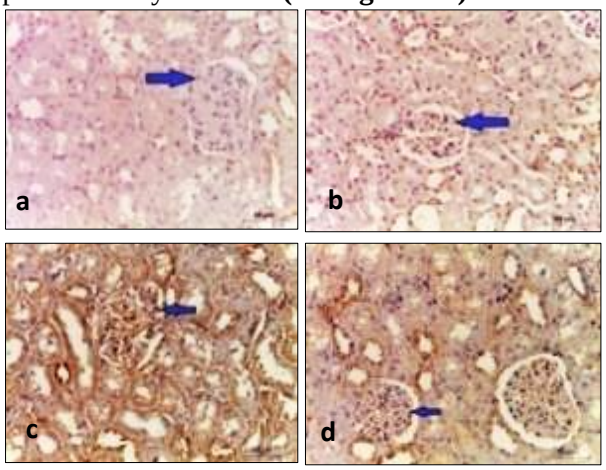

Figure 4: photomicrographs of sections of renal cortex of adult male albino rats**a)**GI,**b)**GII revealing: negative Bax immunoreactivity in glomerular cells (blue arrow), **c**) GIII revealing: strong positive immunoreactivity in glomerular cells (blue arrow) in the form of dark brown granules within the cytoplasm. **d)** GIV revealing markedly reduced immunoreactivity in glomerular cells (blue arrow).**(Avidine-Biotin peroxidase, X400)**

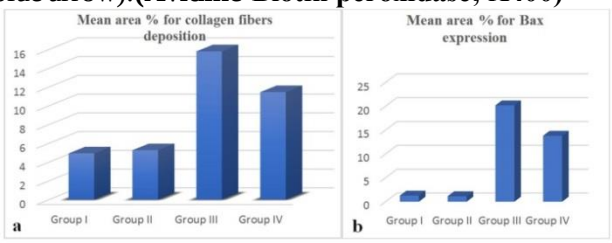

Histogram 3: showing comparison of area % of: **a)** collagen fibers deposition **b)** Bax expression among the four groups.

L/M examination of semithin sections stained with toluidine blue of renal cortex of adult male albino rats of GI and GII revealed, the renal corpuscle (RC) was formed of glomerulus and Bowman's capsule. The glomerular capillaries were lined by endothelium with their nuclei bulging into the lumen and were enveloped by podocytes which had vesicular nuclei. They were supported by centrally located mesangium appeared deeply stained at areas lacking podocytes.The glomerular tuft was separated from parietal layer of Bowman's capsule by the urinary space **(Figure 5a, b)**.While, in GIII some glomerular capillaries showed endocapillary hypercellularity; lymphocyte **(Figure 5c)** and neutrophil**(Figure5f)**.They also showed heterogeneous pattern **(Figure 5c, d)**; together with mesangial changes **(Figure 5c-e)**. Features of podocyte detachment and reinforcement were noticed **(Figure 5d-f)**.There was close apposition between glomerular tuft and Bowman's capsule i.e. apposition of visceral to parietal epithelium **(Figure 5e)** with mitosis among epithelium of the parietal layer **(Figure 5f)**. In GIV, these glomerular changes were ameliorated as compared to GIII **(Figure 5g)**.

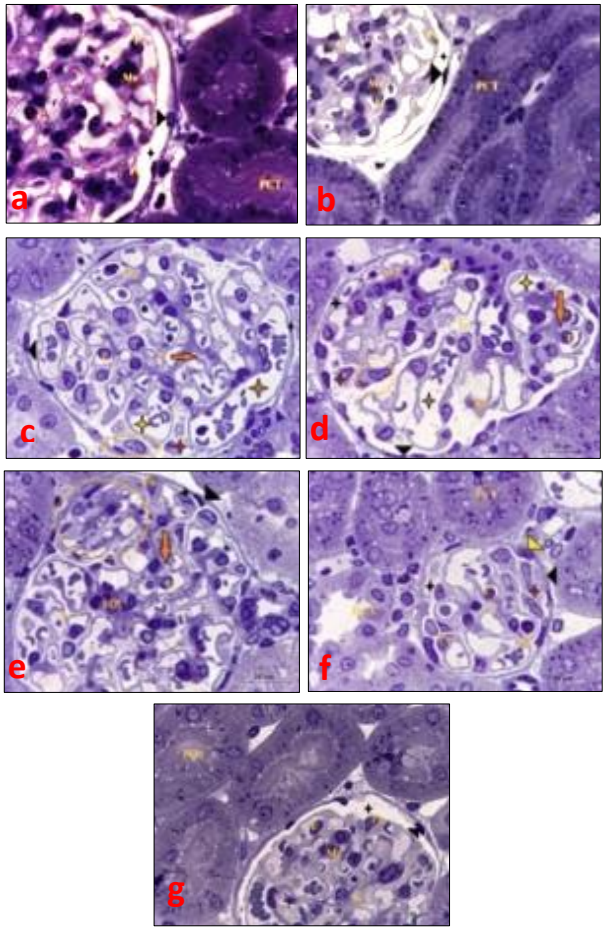

Figure 5: photomicrographs of semithin sections of renal cortex of adult male albino rats **a)** GI, **b)** GII revealing part of the renal corpuscle and proximal convoluted tubules (PCT). Glomerular tuft of capillaries (G), endothelium (E), podocyte (Po), mesangium (Me), parietal layer (black arrow head) and urinary space (black star). **Figures c-f)** GIII**: c-e)** revealing: close apposition (black star), heterogeneous pattern of glomerular capillaries; dilated glomerular capillary (brown star) in relation to other (yellow star), podocyte detached within the urinary space (red star) and another one close to parietal layer of Bowman's capsule (yellow circle). Notice, focal discontinuation of mesangial cell-GBM (orange arrow), and lymphocyte within capillary lumen (Ly) are also illustrated. **d)** Notice, bottle-shaped podocyte (Bo) and vascular pole (Vp). **e)** Notice, some podocytes are close to each other and they apposes to Bowman's capsule (yellow circle) and focal area of mesangial expansion (ME). **f)** Notice, some podocytes become detached and aggregates within the urinary space (red star), neutrophil within capillary lumen (Nt), and mitosis among epithelium of parietal layer (yellow arrow head). ***g)*** GIV revealing: reduced glomerular changes mostly resemble GI, GII. **(Toluidine blue, X1000).**

E/M findings: Ultrastructural study of GI and GII revealed that the glomerular capillaries were lined by fenestrated endothelial cells and their nuclei and perinuclear area bulging into the lumen. They were coated by podocytes which had irregular euchromatic nucleus occupying the cell body. The cell body had major processes and anchoring foot processes. The former gave rise to several interdigitating foot processes housing in between filtration slit covered by slit diaphragm and resting on GBM. The GBM appeared with its characteristic three laminae: rara interna, centrally located lamina densa and rara externa. The subpodocytic space beneath the cell body and the urinary space external to podocyte were noticed **(Figure 6a-d)**.

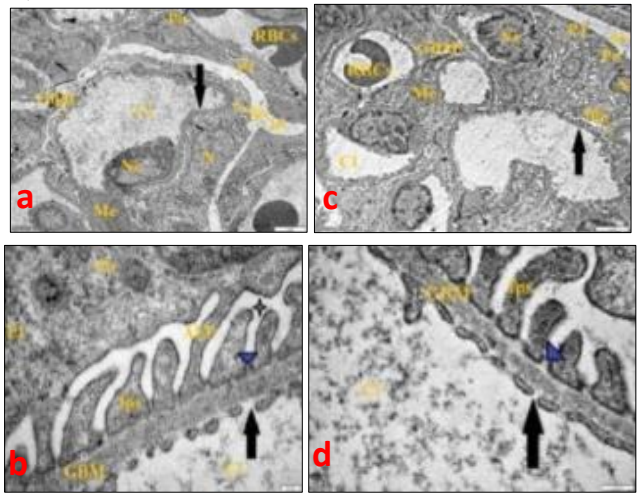

Figure 6: electron micrographs of kidney ultrathin sections of adult male albino rats **a, b)** GI and **c, d)** GII revealing part of the RC. **a, c)** podocyte (Po), euchromatic nucleus (N), major processes (P1), foot processes (fps), trilaminar glomerular basement membrane (GBM).Notice, patent glomerular capillaries lumen (Cl),fenestrated endothelium (arrow), with euchromatic nucleus (Ne),red blood corpuscles (RBCs), mesangium (Me) and urinary space (us). **b, d)** anchoring foot processes (AFP) resting on trilaminar GBM, subpodocytic space (green star) and slit diaphragm (blue arrow head); (**a, c X3000**; **b, d X40,000**).

While in GIII, the glomerular capillaries showed patchy thickening, loss of endothelial fenestrations and capillary expansion. They were in close apposition to Bowman's capsule. Features of podocyte adaptation to stress were noticed. Foot processes showed either variable degree of effacement or detached leaving behind bare area that at some regions denuded segment of GBM was detected. The filtration slit was sealed and the slit diaphragm was displaced, preserved, or lost. The GBM had its usual characteristic three laminae. The subpodocytic space beneath the cell body was focally expanded **(Figure 7a-h)**.

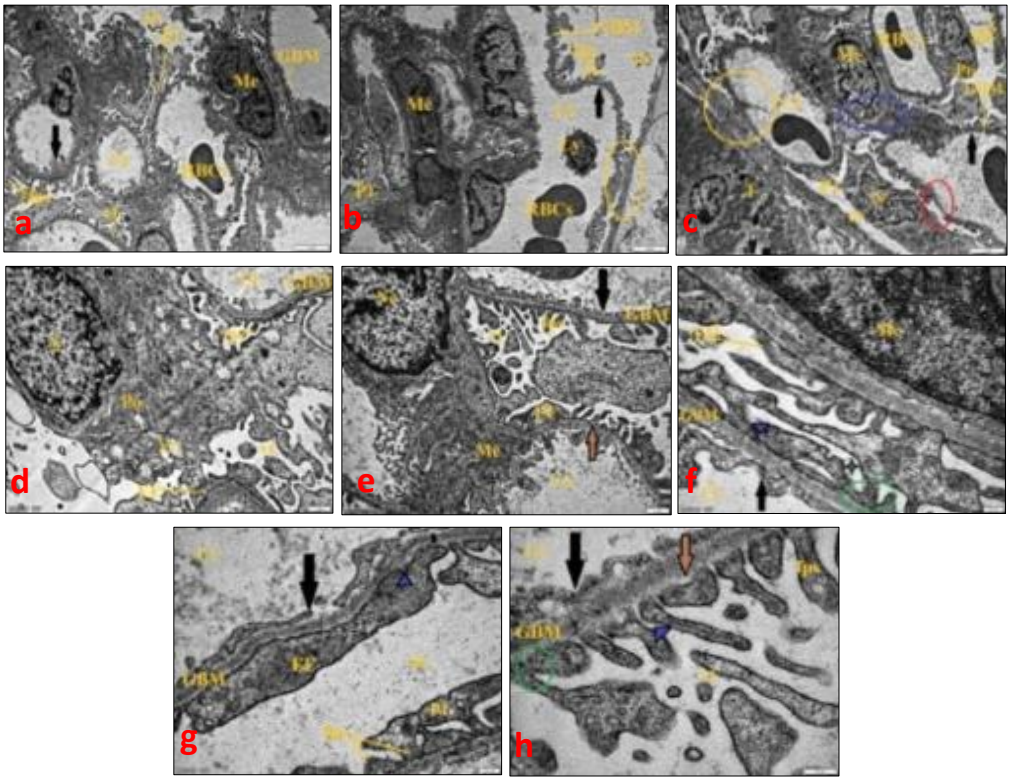

Figure 7: electron micrographs of kidney ultrathin sections of adult male albino rats **a-h)** GIII revealing: part of the RC. **a-c)** patent glomerular capillaries (Cl), endothelium with focal thickening and loss of fenestrations (arrow), stretching of major processes (P1),subpodocytic space expansion (green star), foot processes (fps) resting on trilaminar GBM, mesangium (Me), red blood corpuscles (RBCs), and urinary space (us). **b)** Notice, expanded glomerular capillary (Cl), glomerular apposition to Bowman's capsule (yellow circle), mesangial rearrangement (Me), and lymphocyte (Ly) within the lumen. ***c*)** Notice, podocyte (Po) with euchromatic nucleus (N), attenuation of major processes (P1), denuded segment of GBM (red circle) and focal discontinuation of mesangial cell-GBM (blue circle). **d)** Podocyte with microvillus transformation (vt) and multiple vacuoles within the cytoplasm (Vc). **e)** Bare areas (brown arrow). **f)** fps with variable degree of effacement (EF), occluded filtration slit (green circle), displaced slit diaphragm (blue arrowhead), and subpodocytic space (green star). **g)** Notice, patchy extensive effacement (EF) that the major process resets directly upon the GBM. **h)** Focally lost slit diaphragm (blue arrowhead);
(**a-c X3000; d, e X10,000; f, g X25,000; h X40,000**).

In GIV these changes were ameliorated where the glomerular fenestrations were preserved; some of which had diaphragm; except for focal losses in some capillaries, microvillus transformation still focally detected and effacement was not as extensive as GIII. Bare area and lost slit diaphragm were infrequently observed **(Figure 8a-c)**.

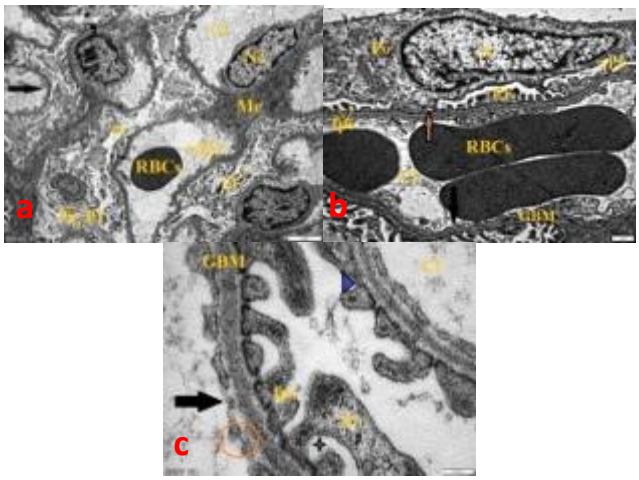

Figure (8): Electron micrographs of kidney ultrathin sections of adult male albino rats ***a-c*)** GIV revealing: part of the RC. **a)** Microvillus transformation (vt), major processes (P1), foot processes (fps), trilaminar GBM, patent glomerular capillaries lumen (Cl), patchy loss of endothelial fenestrations (arrow), endothelium euchromatic nucleus (Ne), red blood corpuscles (RBCs), mesangium (Me), and urinary space (us). **b)** Podocyte (Po) with euchromatic nucleus (N), anchoring foot processes (AFP), focal effacement (EF), subpodocytic space (green star), and bare area (brown arrow). **c)** Fenestrated endothelium with diaphragm (orange circle), and focally obscured slit diaphragm (blue arrowhead).
(**a X3000; b X10,000; c X40,000**).

DISCUSSION

EMB is a biopesticide widely used in crop protection and of choice in salmon fish farms [13].We used aqueous GNE because it has more effective scavenging and chelating power than ethanolic extract[14] . The whole extract was used to avoid the possible mutagenicity of gingerols and shogaols [15]. The obtained GN through milling was homogenous with some agglomerations due to high fibre content of ginger and enhanced fine particle agglomeration during milling process [5].In the current study, there was an insignificant decrease in the mean final BW in GIII in comparison to other groups. This is in agreement with results of **Khaldoun-Oularbi *et al*** [8] who noticed a significant decrease in BW among Wister rats with high dose (10mg/kg/day) and with results of **Gabr *et al.*** [16] who reported that the dose of EMB was directly proportionate to the rate of BW loss. Our results also revealed a significant increase in mean final sCr and BUN in GIII which was improved in GIV, These findings are in accordance with a previous study carried on other AVM analogues [17].It can be explained by diminished cell energy that would be enough only to maintain cell viability but not function. It can also be attributed to reduced glomerular filtration rate and tubular secretion by organic cation transporter/ organic anion transporter as reported by **Vallon**[18].Our observations are also in agreement with those of **Ali *et al.*** [19] who noticed a significant decrement in renal indices in rats concomitantly treated with ginger extract in cisplatin nephrotoxic model. They ascribed this amelioration to the naturally occurring ginger compounds; 6-gingerol and 6-shogaol; that directly scavenge free radicals and indirectly enhance transcription of cytoprotective antioxidant e.g. glutathione (GSH) and superoxide dismutase (SOD).In the present study, there was a significant increase in area % of collagen fibres deposition which was in agreement with those of **Ali *et al.***[19]. We also noticed increased Bowman's capsule thickness in renal corpuscles even when adhesions were absent which was in agreement with results of **Rasch *et al.*** [20]. Our results are supported by results of **Nakamura *et al.*** [21] who suggested fibrosis especially at early stage to be protective and mechanically supportive mechanism providing a three dimensional architecture that supports the remaining functioning nephrons until repair process is complete. These changes were accompanied by significant Bax protein expression in renal cortical tissue in comparison to control groups and GIV, which is in agreement with results of **Yun *et al.***[22] who reported EMB to be the most cytotoxic among 13 tested insecticides being capable of induction of apoptosis and necrosis. These findings were further explained by examining semithin sections of GIII stained with toluidine blue where, some of glomerular capillaries showed endocapillary neutrophil and lymphocyte; a lesion suggestive of endothelial injury in response to podocyte insult, probably via reactive oxygen species (ROS) that are also reported to have role in chemotaxis, and mimicking cellular variant of focal segmental glomerulosclerosis [23]. However, it was not marked probably due to the immunosuppressive properties of AVMs reported by **Eissa and Zidan** [24]. We also noticed heterogeneous pattern of some glomerular capillaries together with mesangial changes; which may represent diminished mesangial stability with either retraction of mesangium into more axial clusters-giving false impression of focal mesangial expansion-or mesangial expansion as compensatory/reconstructive reaction secondary to primary injury as explained by [25]. Although not clear, the mechanism of reduced mesangial stability can be attributed to the effect of ROS either via matrix degradation or via increasing vascular permeability, hence, increasing transmesangial fluid filtration [26]. We also detected some podocytes expressing morphological changes that resembled that described by **Kriz and Lemley** [25] as maladaptive response to stress. The observed aggregated podocytes within the urinary space had another two differentials, either "true" crescent of glomerulonephritis or "pseudocrescent" of collapsing variant of focal segmental glomerulosclerosis with preference of the latter for the cells being adjacent to/on the tuft. The debate is basically about podocytes; being post-mitotic they cannot divide, however, in collapsing glomerulopathy the expression of cyclin-dependent kinase inhibitor $p27^{kip1}$ was found to be lost thus podocytes dedifferentiate and proliferate [23]. The detected close apposition to Bowman's capsule precedes development of adhesions that tend to involve the whole lobule and considered to be preliminary to sclerosis as described by **Nagata *et al.***[27]. The revealed mitosis among epithelium of parietal layer of Bowman's capsule is being quite rare in healthy kidney [28]. Studying glomerular ultrastructure of GIII further revealed, glomerular endothelium changes, which denotes endothelium injury and was similar to that induced by cyclosporine where direct toxic mechanism [29]. We further observed podocyte dynamic changes by which podocyte attempts to resist detachment by adhering to GBM and/or parietal basement membrane as discussed by another authors[25, 28], as well as changes to cope with capillary expansion or fill the gap left behind detached podocytes [27].The noticed foot processes effacement (FPE) was probably due to loss of repulsion between adjacent fps following damage to glomerular polyanions -i.e. matrix and adhesion proteins- via ROS and actin microfilaments reconfiguration [30]. FPE is an attempt either to localize injury or to maintain filtration barrier, and though considered protective, FPE would compromise the overall available filtration surface area leading to compensatory hyperfiltration in other

nephrons as discussed by **Kriz and Lemley** [25]. The observed loss of slit diaphragm and/or sealed filtration slit could be attributed to altered slit diaphragm component probably nephrin, it was reported to be responsible for central filament component observed by E/M [31]. According to [25] sealing of filtration slit is a compensatory mechanism in attempt to maintain lateral stabilization which on its loss retraction of fps leaving GBM bared, disruption of filtration barrier, uncontrolled filtration and expansion of subpodocytic space(SPS) will develop. The retraction/detachment of fps could be due to effect of ROS on adhesion molecules, inability of podocyte to be consistent with the ongoing tuft expansion or rising SPS tension; the sum of which eventually drag podocyte towards urinary pole [25,27,30]. As podocyte attempts to resist detachment it tends to build up cell-to-cell contact a step considered to be irreversible insult and may itself contribute to pseudocyst formation via obstructing the SPS draining channels adequately explained by many authors [25,27]. Our distinguished ultrastructural changes are in accordance with those of **Daehn *et al.*** [32] who suggested a cross-talk between podocyte and glomerular endothelium. They also reflect the ability of EMB to disturb glomerular structure probably via affecting different cells. On studying L/M sections of GIV we observed markedly reduced area % of collagen fibres deposition as well as markedly reduced area % of Bax protein expression in renal cortex as compared to GIII. Our results coincide with the ameliorative effect of ginger extract previously reported by **Ali *et al.*** [19] who observed diminished morphological and immunohistochemical changes in cisplatin nephrotoxic model. These findings were confirmed by studying semithin sections of GIV stained with toluidine blue where, glomerular changes were reduced that it mostly resembled control groups. Ultra-structurally, the glomerular changes were not as extensive as EMB group. We also noticed glomerular fenestrations with diaphragm which is in accordance with results of **Ichimura *et al.*** [33] who assumed it to be part of post-damage reconstruction. Our observations are supported by results of **Binder *et al.*** [34] who reported potential protective effect of antioxidants against glomerular morphological changes probably due to preservation of glomerular polyanions. In this context, **Brezniceanu *et al.*** [35] assumed that induction of endogenous antioxidants via polyphenols would be more promising than the use of exogenous antioxidants-e.g. vitamin E-for they act within the cell or cellular compartment where ROS are actually generated.

CONCLUSION

EMB affected different cell components of the renal corpuscle and aqueous GNE has an ameliorative effect probably due to its antioxidant activity that provided protection for renal tissue together with better kidney function tests.

REFERENCES

1-Ouyang W, Cai G, Huang W *et al.* (2016): Temporal-spatial loss of diffuse pesticide and potential risks for water quality in China. Science of the Total Environment, 541:551-558.

2-Luan S, Muhayimana S, Xu J *et al.* (2019): The effect of α-tocopherol and dithiothreitol in ameliorating emamectin benzoate cytotoxicity in human K562 cells involving the modulation of ROS accumulation and NF-κB signaling. Ecotoxicology and Environmental Safety, 167:114-121.

3-Valcke M, Levasseur M-E, da Silva AS *et al.* (2017): Pesticide exposures and chronic kidney disease of unknown etiology: an epidemiologic review Sweden. Environmental Health, 16:49-52.

4-da Silveira Vasconcelos M, Mota EF, Gomes-Rochette NF *et al.* (2019): Ginger (*Zingiber officinale Roscoe*). In: Nonvitamin and Nonmineral Nutritional Supplements. Eds. Nabavi, S.M. and Silva, A.S.:pp.235-239.

5-Norhidayah A, Noriham A and Rusop M (2013): Antioxidant property of dry and wet mill nanostructured *Zingiber officinale Rosc*. (Ginger) rhizome: a comparative study. IPCBEE., 55:112-116.

6-El-Sheikh E and Galal A (2015): Toxic effects of sub-chronic exposure of male albino rats to emamectin benzoate and possible ameliorative role of Foeniculum vulgare essential oil, Environmental Toxicology and Pharmacology, 39:1177-1188.

7-Ogino M, Yakushiji K, Suzuki H *et al.* (2018):Enhanced pharmacokinetic behavior and hepatoprotective function of ginger extract-loaded supersaturable self-emulsifying drug delivery systems. Journal of Functional Foods, 40:156-163.

8-Khaldoun-Oularbi H, Allorge D, Richeval C *et al.* (2015): Emamectin benzoate (Proclaim®) mediates biochemical changes and histopathological damage in the kidney of male Wistar rats (Rattus norvegicus). Toxicologie Analytique and Clinique, 27:72-80.

9-Kiernan JA (2015): Histological and histochemical methods: Theory and Practice. 5th ed., Scion Publishing Ltd.

10-Marzo I,Brenner C, Zamzami N *et al.* (1998): Bax and adenine nucleotide translocator cooperate in the mitochondrial control of apoptosis. Science, 281: 2027–2031.

11-Ragab A H (1970): The structure and innervation of tortoise muscle spindles. Ph.D. Thesis, Univ. of Durham, U.K.

12-Diaz Encarnacion MM, Griffinb MD, Slezakc JM *et al.* (2003): Correlation of quantitative digital image analysis with the glomerular filtration rate in chronic allograft nephropathy. American Journal of Transplantation, 4:248-256.

13-Parsaeyan E, Saber M and Bagheri M (2013): Toxicity of emamectin benzoate and cypermethrin on biological parameters of cotton bollworm, *Helicoverpa armigera* (Hubner) in laboratory conditions. J. Crop Protect., 2:477-485.

14-Yeh HY, Chuang CH, Chen HC *et al.* (2014): Bioactive components analysis of two various gingers (Zingiber

officinale Roscoe) and antioxidant effect of ginger extracts. LWT-Food Science and Technology, 55(1):329-334.

15-Nagabhushan M, Amonkar AJ and Bhide SV (1987): Mutagenicity of gingerol and shogaol and antimutagenicity of zingerone in salmonella/microsome assay. Cancer Letters, 36(2):221-233.

16-Gabr GA, Soliman GA, Abdulaziz SS *et al.* (2015): Teratogenic effects in rat fetuses subjected to the concurrent in utero exposure to emamectin benzoate insecticide. Pakistan Journal of Biological Sciences, 18(7):333-340.

17-Meligi NM and Hassan HF (2017): Protective effects of Eruca sativa (rocket) on abamectin insecticide toxicity in male albino rats. Environ Sci Pollut Res., 24:9702-9712.

18-Vallon V (2016): Tubular transport in acute kidney injury: relevance for diagnosis, prognosis and intervention. Nephron, 134:160-166.

19-Ali DA, Abdeen AM, Ismail MF *et al.* (2015): Histological, ultrastructural and immunohistochemical studies on the protective effect of ginger extract against cisplatin-induced nephrotoxicity in male rats. Toxicology and Industrial Health, 31(10):869-880.

20-Rasch R, Nyengaard JR, Marcussen N *et al.* (2002): Renal structural abnormalities following recovery from acute puromycin nephrosis. Kidney International, 62:496-506.

21-Nakamura J, Sato Y, Kitai Y *et al.* (2019): Myofibroblasts acquire retinoic acid-producing ability during fibroblast-to-myofibroblast transition following kidney injury. Kidney International, 95:526-539.

22-Yun X, Huang Q, Rao W *et al.* (2017): A comparative assessment of cytotoxicity of commonly used agricultural insecticides to human and insect cells. Ecotoxicology and Environmental Safety, 137:179-185.

23-Fogo AB and Kashgarian M (2017): Diagnostic Atlas of Renal Pathology. 3rd ed., Philadelphia, PA: Elsevier.

24-Eissa FI and NA Zidan (2009): Haematological, biochemical and histopathological alterations induced by abamectin and bacillus thuringiensis in male albino rats. Australian Journal of Basic and Applied Sciences, 3(3):2497-2505.

25-Kriz W and Lemley KV (2017): Mechanical challenges to the glomerular filtration barrier: adaptations and pathway to sclerosis. Pediatric Nephrology, 32(3):405-417.

26-Eberhardt W, Huwiler A, Beck K-F *et al.* (2000): Amplification of IL-1b-induced matrix metalloproteinase-9 expression by superoxide in rat glomerular mesangial cells is mediated by increased activities of NF-kb and activating protein-1 and involves activation of the mitogen-activated protein kinase pathways. The Journal of Immunology, 165:5788-5797.

27-Nagata M, Scharer K and Kriz W (1992): Glomerular damage after uninephrectomy in young rats. I. Hypertrophy and distortion of capillary architecture. Kidney International, 42:136-147.

28-Le Hir M, Keller C, Eschmann V *et al.* (2001): Podocyte bridges between the tuft and bowman's capsule: an early event in experimental crescentic glomerulonephritis. Journal of American Society Nephrology, 12:2060-2071.

29-Kobayashi M, Takaya S, Koie H *et al.* (1991): Glomerular endothelial changes in cyclosporine a-treated rats: scanning and transmission electron microscopic studies. Japanese Journal of Surgery, 21(2):210-215.

30-Kojima K, Davidovits A, Poczewski H *et al.* (2004): Podocyte flattening and disorder of glomerular basement membrane are associated with splitting of dystroglycan–matrix interaction. J Am Soc Nephrol., 15:2079-2089.

31-Rodewald R and Karnovsky MJ (1974): Porous substructure of the glomerular slit diaphragm in the rat and mouse. The Journal of Cell Biology, 60:423-433.

32-Daehn I, Casalena G, Zhang T *et al.* (2014): Endothelial mitochondrial oxidative stress determines podocyte depletion in segmental glomerulosclerosis. J Clin Invest., 124(4):1608-1621.

33-Ichimura K, Stan RV, Kurihara H *et al.* (2008): Glomerular endothelial cells form diaphragms during development and pathologic conditions. Journal American Society of Nephrology, 19:1463-1471.

34-Binder CJ, Weiher H, Exner M *et al.* (1999): Glomerular overproduction of oxygen radicals in MPV17 gene-inactivated mice causes podocyte foot process flattening and proteinuria a model of steroid-resistant nephrosis sensitive to radical scavenger therapy. Am J Pathol., 154:1067-1075.

35-Brezniceanu ML, Liu F, Wei CC *et al.* (2008): Attenuation of interstitial fibrosis and tubular apoptosis in db/db transgenic mice overexpressing catalase in renal proximal tubular cells. Diabetes, 57:451-459.